Bioorganic Chemistry 84 (2019) 63–75

Contents lists available at ScienceDirect

Bioorganic Chemistry

journal homepage: www.elsevier.com/locate/bioorg

Switching of Trp-214 intrinsic rotamer population in human serum albumin: An insight into the aftermath of embracing therapeutic bioorganic luminophore azapodophyllotoxin into sudlow site I

Soham Mukherjee[a], Kapil Ganorkar[a], Ajay Kumar[b], Naina Sehra[a], Sujit Kumar Ghosh[a,*]

[a] Department of Chemistry, Visvesvaraya National Institute of Technology, Nagpur, Maharashtra 440010, India
[b] International Centre for Trans-disciplinary Research, School of Environmental Affairs, Universidad Metropolitana, PR 00928, United States

ARTICLE INFO

Keywords:
Azapodophyllotoxin
Human serum albumin
FRET
Time-resolved fluorescence
Fluorescence anisotropy
Molecular docking

ABSTRACT

Human serum albumin is perceived to be the most abundant protein in human blood plasma and functions as a major carrier of different enzymes and drugs inside human body. The present article puts in an effort to demonstrate the attitude adopted by human serum albumin towards a potential therapeutic luminophore 4-(2-Hydroxyethyl)-10-phenyl-3,4,6,7,8,10-hexahydro-1H-cyclopenta[*g*]furo[3,4-b]quinoline-1-one (HPFQ). HPFQ is a prodigy from azapodophyllotoxin class of compounds, which have been synthesized from the perspective of improved bioactivity than its prologue podophyllotoxins. While, HPFQ has proved to be highly bioactive against most cancer cell lines with best GI_{50} values of < 0.1 μM for a major number of cell lines; it also showed terrific fluorescent properties throughout the polarity scale, worthy of a promising imaging agent. The binding mechanism of HPFQ with HSA has been established by combining *in vitro* spectroscopic techniques, *in silico* molecular docking and induced fit docking (IFD). The competitive site-binding studies demonstrated that the otherwise anion-receptor sudlow site I of HSA nurtures neutral HPFQ with prudent affinity (Binding constant, $K_b = 0.74 \times 10^5\,M^{-1}$). The time-resolve fluorescence studies reveal an appreciable reduction in HSA average radiative lifetime against an increase in HPFQ concentration and provided evidence for Forster's resonance energy transfer (FRET) being responsible for the dominant quenching mechanism, escorted by minor structural deformations in the backbone of protein structure. HPFQ institutes itself near Trp-214 within protein matrix, and subsequently the "hydrophobic amino acids" dominated cybotactic environment of Trp-214 experiences a reduction in the micropolarity. The allosteric modulation triggered by the stronger association of HPFQ with HSA leads towards minor deformation in secondary structure of protein. Sudlow site I of HSA proficiently embraces a favourable conformation like malleable dough to furnish space for arriving bioactive HPFQ molecule. HPFQ is also believed to administer the conformational regulation in HSA domain by affecting inter-conversion of HSA rotamers, which may prove to be an enlightening area to decode the preferable interaction between them. The juxtaposed spectroscopic research described herein is expected to embolden design of azapodophyllotoxin based anti-proliferative clinical agents for efficient *in vivo* bio-distribution employing HSA-centred drug delivery and administration systems.

1. Introduction

During the process of new drug analysis, the interaction between drugs and plasma proteins yields crucial information about the pharmacokinetic portfolio of novel compounds [1–3]. Such interactions are accountable for unswerving manipulation of drug's concentration in human blood and at its binding sites, thus subsequently contributing to its extent of biotransformation and toxicological action *in vivo*. Subsequently, exploration of pharmacokinetics of novel drugs in human plasma might prove to be fascinating for exquisite analysis of drug-protein interaction [4–6]. Human serum albumin is one of the most developed protein having two distinct features preserved throughout its domains and different species: the highly helical secondary structure and the tertiary structure, containing the typical arrangement of disulfide bridges, constitute a significant facet of protein stabilization [7].

HSA is a well-recognized transport protein, associated with disposition of different drugs and relevant molecules [8,9]. A symmetric fatty acid distribution in HSA allows it to demonstrate excellent

* Corresponding author.
E-mail address: skghosh@chm.vnit.ac.in (S.K. Ghosh).

https://doi.org/10.1016/j.bioorg.2018.11.015
Received 6 September 2018; Received in revised form 2 November 2018; Accepted 13 November 2018
Available online 16 November 2018
0045-2068/

conformational adaptability and flexibility towards binding various molecules [2].

In the context of spectroscopic characteristics, HSA has only one Trp residue (Trp-214), which is pivotal for the fluorescent emission produced from protein matrix [10]. The modulation in microenvironments surrounding the Trp residue can generate significant alteration in protein intrinsic fluorescence properties [4,5,11,12], and thus the investigation about their interactions with novel pharmacophores can yield valuable insights to decode the environment sensitive molecular interactions [13].

The Trp residue of HSA, owing to highly sensitive indole side chain, has proved to be the most popular fluorescent probe for investigation of conformation and dynamics of the receptor protein [14]. The modulation in the Trp fluorescence spectra are often observed in response to protein conformational switching, or other molecular association. The dominating fluorophore Trp exhibits appreciable emission around 310–350 nm region (while excited at corresponding absorption peak) and also displays multi-exponential decay with excited state lifetime oscillating from 50 ps to 8 ns. This multi-exponential fluorescence decay may be accredited to the different ground state conformers, which are usually explained by the classically accepted rotamer (rotational conformer) model. To be more precise, the Tryptophan rotamerisation emerges from the rotation of indole ring about Cα-Cβ bond or Cβ-Cγ bond. The rate of this inter-conversion happens to be so fast that it can only be seized within faster time scale [15–17]. The rotamers exist with different decay times, diverse pathways and varied rate of depopulation of excited state. The distinct lifetime of such rotamers bears physical immense significances as the pre-exponential factors are proportional to the relative population of each rotamer present, and the decay time constants are governed by the surrounding microenvironment of each rotamer. The TRF of receptor HSA is sensitive towards the binding molecule as it may affect the native form of tryptophan residues, or may act as quenchers or energy acceptor in resonance energy transfer process. The extent of interaction between the fluorescing tryptophan residue and the bound molecule is directed by the intermediate distance and their relative orientation.

Hence, the populations of different rotamer of Trp in HSA provides useful insights in understanding the detailed mechanistic and functional information about the ligand binding [18]. In this context the interaction of potential dual therapeutic and imaging agent HPFQ with human blood plasma protein may account for serious attention as it can modify the pharmacodynamics and pharmacokinetics of azapodophyllotoxin class of compounds.

The HPFQ molecule is a member of azapodophyllotoxin class of compounds, which are alternative scaffold of proven anti-tumor compound podophyllotoxin [19–21]. The synthesis of these compounds was undertaken with an objective of better anti-tumor activity and lower cytotoxicity towards normal cells. HPFQ has proved to be highly active against most cancer cell lines with GI_{50} values of < 0.1 μM for 50% cell lines and 0.01 μM for 30% cell lines (with LC_{50} value > 25 μM); although it is not selective towards any particular cell line [22]. However, the comprehensive mechanistic investigation for the anti-malignant activity is still under way. HPFQ also exhibited vastly intense fluorescent emission along the entire polarity scale by the virtue of underlying intramolecular charge transfer (ICT) state and extensive H-bond network, which proves it to be quite unique from the perspective of imaging capability [23]. Hence, the investigation towards binding interaction of HPFQ with HSA becomes especially significant as, its transportation mechanism is governed by the conformational malleability and flexibility of receptor protein to promote the interaction with the visitant (HPFQ) [24]. Simultaneously in this present work, we have investigated the binding interaction of a potent dual therapeutic and imaging agent with transport protein HSA under controlled physiological conditions by adapting combined approach of *in vitro* optical spectroscopic techniques like steady-state UV–Visible absorption, steady-state fluorescence emission and anisotropy, time resolve fluorescence along with *in silico* molecular docking and IFD study employing the Schrödinger suite. The work helps to reveal the hidden scenario behind binding pattern and affinity of HPFQ towards HSA, and also demonstrate how the compound is able to interact with the rotamers of HSA and regulate their contribution.

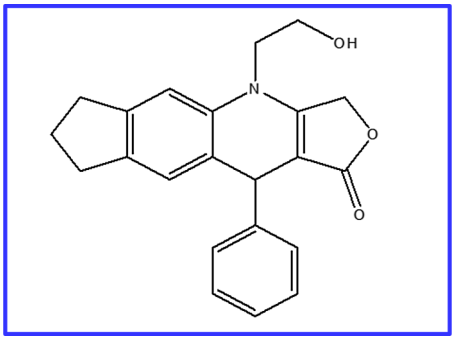

Scheme 1. Structure of HPFQ.

2. Experimental section

2.1. Materials

The therapeutic HPFQ (Scheme 1) molecule has been synthesized (ESI Scheme S1) as informed elsewhere [22]. HSA is obtained from Sigma Aldrich (USA). HEPES buffer is obtained from SRL, India and used as received. Ibuprofen and Warfarin are procured from Bangalore Fine chemicals, India. Stock solutions of HSA and Warfarin are prepared using 10 mM HEPES buffer of pH 7.0 and subsequently stored at 4 °C. Concentrated stock solutions of HPFQ and Ibuprofen are prepared in spectroscopic grade 1,4-dioxane and stored at 4 °C. Millipore water is used as per requirements during the experiments.

2.2. Instrumentation and methodology

2.2.1. Steady-state UV–Visible absorption measurements

The measurements were undertaken using JASCO V-630 Spectrophotometer, operational with a Peltier temperature control system. All the steady-state absorption spectra were collected by exploiting a synchronized pair of quartz cuvettes with path length of 10 mm.

2.2.2. Steady-state fluorescence

The fluorescence spectra measurements are undertaken by JASCO FP-8300 spectrofluorometer, armed with a thermostatically controlled cell holder (which remains attached with a water bath and maintains required temperature). All spectra are recorded with quartz cuvettes of 1.0 cm path length. The slit widths for excitation and emission are fixed at 2.5 nm. In order to detect the fluorescence quenching by HPFQ, selective excitation of the Tryptophan residues are carried out at 295 nm with equilibration time of 3 min. The above procedure at three different temperatures i.e., 293, 298 and 303 K is undertaken to decipher the effect of temperature on HSA-HPFQ binding interaction. The correction due to inner filter effect at the excitation and emission wavelengths of the protein for all fluorescence measurements are undertaken using the following equation [25]:

$$F_{corr} = F_{obs} * antilog\,[(A_{ex} + A_{em}/2)] \quad (1)$$

where F_{corr} and F_{obs} are the rectified and measured fluorescence intensities, respectively, while A_{ex} and A_{em} are the optical density of HPFQ at the respective excitation and emission wavelengths.

2.2.3. Steady-state fluorescence anisotropy

We have exploited JASCO FP-8300 spectrofluorometer to monitor steady state fluorescence anisotropy, at 298 K, with manually operated

perpendicular and parallel emission polarizers, Fluorescence anisotropy (r) is defined as [25]:

$$r = (I_{VV} - GI_{VH})/(I_{VV} + 2GI_{VH}) \quad (2)$$

$$G = I_{HV}/I_{HH} \quad (3)$$

where I_{VV} and I_{HV} are the emission intensities, which are obtained when the excitation polarizer gets oriented vertically while the emission polarizer gets oriented vertically and horizontally, respectively.

2.2.4. Time resolved fluorescence (TRF) measurements

PTI Pico Master TSCPC spectrofluorometer, equipped with a PMH-100-4 detector and a 280 nm LED (as excitation source) is exploited to measure fluorescence lifetimes, while employing the method of TCSPC technique. SDS is used as a scatterer to record the instrument response function with the excitation wavelength kept at 280 nm (± 10 nm) and bandwidths fixed at 2 nm. The data collection and analysis are carried out using the *Felix GX* software. The appropriateness of fit is adjudged by considering combined effects of χ^2 values and visual observations of residuals, fitted line and autocorrelation functions. The fluorescence decay curves are subsequently analyzed by exponential iterative fitting programs of different degrees such as [25]:

$$F(t) = \sum_i \alpha_i \exp(-\tau/\tau_i) \quad (4)$$

where α_i represents a pre-exponential factor which denotes fractional relative contribution to the decay of i-th component with a lifetime τ_i. Average lifetimes τ_f stemming from multi-exponential decays are calculated using pre-exponential factors and decay times in the following equation [25]:

$$\tau_f = \sum \alpha_i \tau_i / \sum \alpha_i \quad (5)$$

2.2.5. Site marker displacement experiments

We carry out site marker displacement experiments using fluorescence titration methods, to recognize the binding site of HPFQ in protein matrix separately, in the presence of two different stereotypical site markers (Warfarin and Ibuprofen). Equimolar concentrations of HSA and site markers are taken and HPFQ is then added gradually. All emission spectra are recorded with an excitation wavelength of 295 nm, at 298 K.

2.2.6. Synchronous fluorescence measurements

The synchronous fluorescence spectra (at constant wavelength) of HSA are recorded with gradual increase in amounts of HPFQ, while being monitored by JASCO FP-8300spectrofluorometer. The spectra are obtained by scanning the samples in the wavelength ranges of 260–340 nm while maintaining $\Delta\lambda$ of 15 nm and in the ambit of 260–370 nm, while maintaining $\Delta\lambda$ of 60 nm. These measurements yield typical information for Tyrosine and Tryptophan microenvironments, respectively within protein matrix.

2.2.7. Circular dichromism spectroscopic measurements

JASCO-J-815 spectropolarimeter is exploited for recording Circular dichromism (CD) spectra at 298 K. A quartz cuvette with path length of 1 cm has been used to carry out the measurements. The reported CD profile is taken as an average of four successive scans with 20 nm per minute while baseline is corrected appropriately over a wavelength range of 260–200 nm. The base line corrected final plots reported herein are taken as an average of three accumulated plots. The α-helix content and the differential were calculated from CD spectra. The observed ellipticity θ has been used in following equation, to calculate the molar ellipticity [θ] as,

$$[\theta] = \frac{100 \times \theta}{c \times l} \quad (6)$$

where c denotes the concentration of the HSA solution in mol dm^{-3} and l represents the path length (in cm) of the cell. The result of CD measurements were expressed as mean residual ellipticity (MRE) in deg·cm^2·$dmol^{-1}$ according to the following equation [26]:

$$\text{MRE} = \text{observed CD (mdeg)}/C_p nl \times 10 \quad (7)$$

where c_p denotes the molar concentration of HSA, n denotes the number of amino acid residues (585), and l denotes the path length (1 cm). The α-helix contents of the native and complexed HSA have been calculated from the MRE value at 208 nm using the following equation [4]:

$$\alpha - \text{helix}\,(\%) = [-\text{MRE}_{208} - 4000/33000 - 4000] \times 100 \quad (8)$$

where MRE_{208} denotes the experimental MRE value at 208 nm while the MRE of the β-form and random coil conformation cross at 208 nm is taken to be 4000 and the MRE value of a pure α-helix is considered to be 33,000 at 208 nm.

2.3. In silico measurements

The *in silico* molecular docking studies are undertaken exploiting a Linux centos 6 operating system, armed with 64 bit Intel ®core™ i5-2500 CPU @ 3.30 GHz and 4 GB RAM. All the studies are accomplished employing the Schrödinger suite 2014 by Maestro.

2.3.1. Preparation of ligand and protein

The crystal structure of HSA (1AO6) and the relevant ligand, HPFQ, are prepared with the assistance of Ligprep [27] and protein preparation wizard.

2.3.2. Recognition of binding site in HSA

The site map identifies active sites and consequently investigates the entirely prepared protein for plausible binding sites. Minimum 15 points per described site are required by site map while a more restraining definition of hydrophobicity is used with setting for standard grid which consists crop sites at a distance of 4 Å from the nearest site point. For first level of approximation, docking has been adopted to determine a list of probable binding sites in HSA and to acquire the binding energy for the protein-ligand complex. Such energy based scoring function comprises of terms which account for very short range Van der Waals forces, electrostatic interactions, Hydrogen bonding interactions and penalty scoring function. The docking calculation yields several conformers of ligand, of which, the complimentarily best one with smallest penalty scores and lowest binding energy against the receptor, is taken up for further analysis.

2.3.3. Molecular docking and induced fit docking

HPFQ is docked at the specific sites acknowledged by site map exploiting XP mode of Glide [28,29]. The most favorable pose of individual ligand in its particular site is selected and further processed for carrying out the flexible docking study using IFD.

3. Results and discussions

3.1. Recognition of the interaction between HPFQ and human serum albumin by exploiting in vitro optical spectroscopic techniques

Human serum albumin is the most critical protein component in human blood due to its ability in binding and carriage of several significant hormones and drug molecules [13]. A bioactive molecule present in blood system, interacts and bind with plasma proteins in a reversible manner, by varying extents. These bindings often bear a signature of pharmacodynamics and pharmacokinetics of the drug. The binding between protein and hydrophilic drug molecule increases molecular solubility in carrier system [30]. Hence, the study of drug's mode and affinity of binding with plasma protein appears to pose immense biophysical importance, which in turn may further assist to

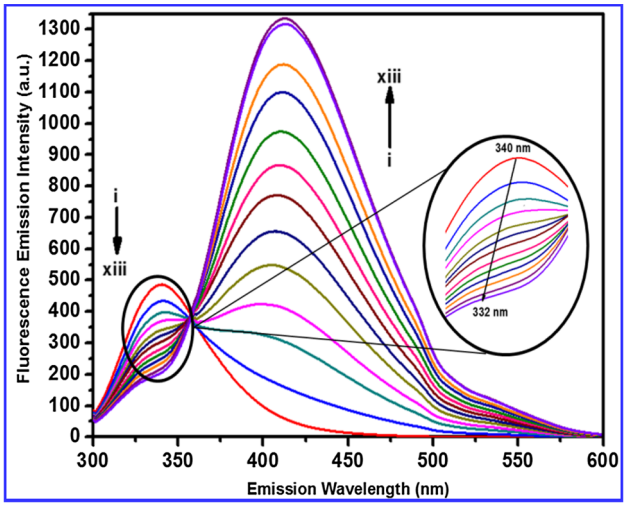

Fig. 1. Emission spectra demonstrating the quenching in intrinsicTrp-214 fluorescence of HSA with gradual increase in concentration of HPFQ. [HSA] = 4.98 μM; i → xiii: [HPFQ] = 0–11.95 μM; T = 298 K; λ_{ex} = 295 nm.

increase efficacy in formulation of novel bioactive molecule.

Here, steady state fluorescence spectroscopy technique has been exploited to monitor the modulation in intrinsic fluorescence of plasma protein by selective photo-excitation of Trp 214 at 295 nm. The wavelength is preferred over 280 nm photo-excitation for tenacious detection of sole Trp 214 emission over collective emission of Trp 214 and 18 Tyr residues present in large hydrophobic pocket of subdomain II A [31]. With the gradual increment of HPFQ concentration in aqueous buffer solution of human serum albumin at physiological pH of 7.4, a gradual decrement has been observed in intrinsic fluorescence emission intensity for HSA (Fig. 1), probably exposing the surrounding environment of naturally hydrophobic amino acid residue to polar contents. An appreciable hypsochromic shift of 8 nm (340 nm to 332 nm) for Trp emission maxima indicates the modulation in local polarization of Trp residue by HPFQ. However, the possibilities of protein denaturation can be ruled out as protein unfolding is believed to expose Trp 214 to aqueous interfaces and thus exhibiting red shift in the emission maxima of Trp 214. These observations about surrounding microenvironment of fluorophore were further supported and unveiled by synchronous fluorescence technique, in later sections.

The interaction of HPFQ with HSA has not only led to quenching of Trp fluorescence, but a subsequent appearance of a band at around 413 nm is observed with its intensity getting enhanced on increasing the concentration of the anti-cancer molecule. The reason behind such event may lie in the fact that HPFQ conquers an appreciable absorption near the protein emission peak at 340 nm. Although, emission profile of HPFQ does not change with that of protein fluorescence. Under such conditions, the novel band appears to originate from a combined contribution of: (i) energy transfer from Trp 214 of proteins to HPFQ and (ii) free HPFQ emission. Nevertheless, the contribution from free HPFQ emission can be nullified by observing its inconsistency, while comparing with that of free HPFQ in pure aqueous system. HPFQ does not show appreciable absorption in the region of Trp absorption (295 nm) and its emission (while being excited at 295 nm) appears to be merely meager while compared to its normal emission. It might be significant to mention that, with gradual blue shift in Trp 214 emission of HSA, the emission intensity of 413 nm peak also increases; which insists towards the energy transfer between donor Trp 214 and acceptor HPFQ. The gradual dominance of 413 nm peak might be due to the gradual approach of Trp 214 fluorescence emission maxima towards absorption maxima of HPFQ (~328 nm). This, in turn, enhances effective relocation of energy from donor to acceptor and expresses by exhibition of higher emission intensity at that region. The shift in that region, compared to solvatochromic studies (ESI Fig. S1) of free HPFQ [23], reveal the change in polarity of surrounding environment of the HPFQ in globular proteins.

3.2. Revelation of binding affinity and quenching mechanism exhibited by HPFQ-HSA system

The increased hydrophobicity around the Trp-214 fluorophore is manifested by the blue shift in its emission maxima, whereas the progressive decrement of the tryptophan fluorescence by HPFQ suggests its binding interaction with the host protein molecule [32–35]. A diverse range of molecular interactions can play important role in fluorescence quenching. Some of these phenomena are excited-state interactions, molecular rearrangements, energy-transfer processes etc [36,37]. Dependence on variation in temperature or measurements of radiative lifetime facilitate us to distinguish between the incidence of dynamic and static quenching. So, in order to quantify the fluorescence quenching phenomena, involved between HPFQ and the globular protein system, the recognized Stern-Volmer (SV) analysis is exploited to the fluorescence quenching observed at different temperatures using the following SV equation [25]:

$$\frac{F_0}{F} = 1 + K_{sv}[Q] = 1 + k_q \tau_0 [Q] \tag{9}$$

where F_0 and F are the steady-state fluorescence intensities of globular proteins in the absence and presence of HPFQ, respectively, K_{sv} is the Stern-Volmer quenching constant, and $[Q]$ is concentration of quencher HPFQ, k_q is bimolecular quenching constant and τ_0 is the average lifetime of the protein in the absence of quencher HPFQ. Here, τ_0 has been considered to be 1×10^{-9} s for the determination of k_q values at different temperatures. Here, inner filter effect has been taken care of, to correct the fluorescence spectra with respect to absorption of quencher at the excitation and emission wavelengths of the fluorophore. The maximum bimolecular collision quenching constant for various quenchers with biomolecules is found to be 2.0×10^{10} L mol^{-1} s^{-1} [38–41]. In this case, the Stern-Volmer plot in lower concentration appears to be a straight line with a very high k_q value (of the order 10^{14}), which may indicate involvement of static quenching via ground state complex formation (Table 1). Although, TRF measurements (discussed later) show that subsequent dynamic quenching process is also present in the interaction between HPFQ and protein systems, which is evident from biphasic nature or positive curvature observed in Stern-Volmer plot [42] (higher concentration range coupled with lower range) (Fig. 2).

Moreover, diminution in K_{sv} values at elevated temperatures indicates towards optimal affinity of HPFQ toward the plasma protein, which may prove to be advantageous for diffusion of bioactive molecule to target sites from the transport system. The quenching patterns suggest a similar binding association of HPFQ with HSA and points towards perturbation of secondary structure of plasma proteins.

The following double-logarithmic equation can be exploited for static quenching interactions, in order to find out the binding constant and the number of binding sites [25]:

$$\log\left(\frac{F_0 - F}{F}\right) = \log K_b + n \log [Q] \tag{10}$$

Table 1
Quantification of quenching parameters of HPFQ-HSA interaction at different temperatures:

Temp (K)	K_{sv} (10^5 L mol^{-1})	k_q (10^{14} L mol^{-1} s^{-1})	R[a]
293	1.703 ± 1.78%	1.703 ± 3.22%	0.989
298	1.486 ± 2.68%	1.486 ± 2.42%	0.993
303	1.291 ± 3.39%	1.291 ± 2.04%	0.986

R[a] denotes the correlation factor for the modified Stern-Volmer plots.

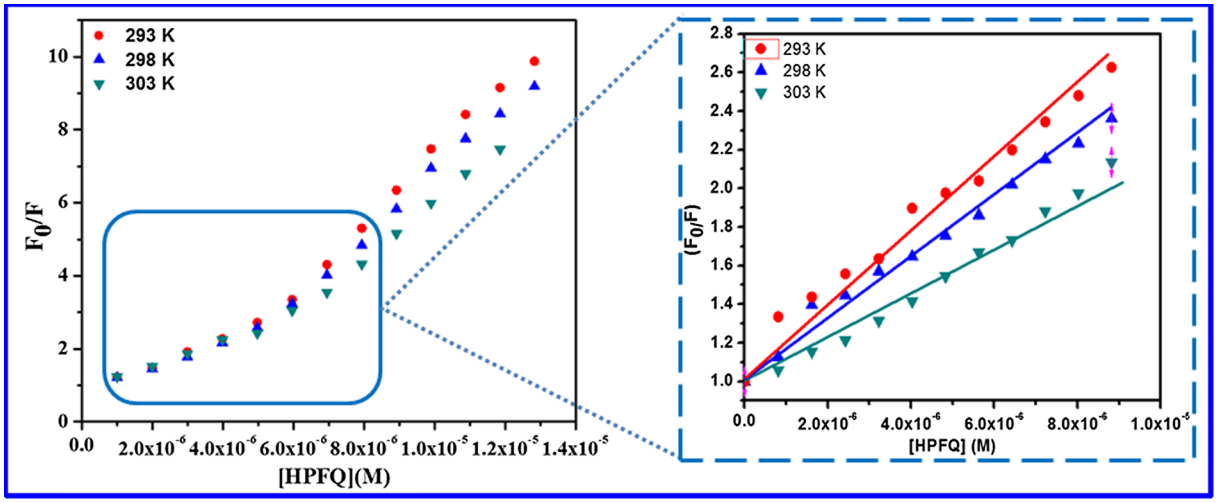

Fig. 2. Corrected Stern-Volmer Plots for the interaction between HPFQ and HSA at different temperature: (A) Full concentration range and (B) lower concentration range.

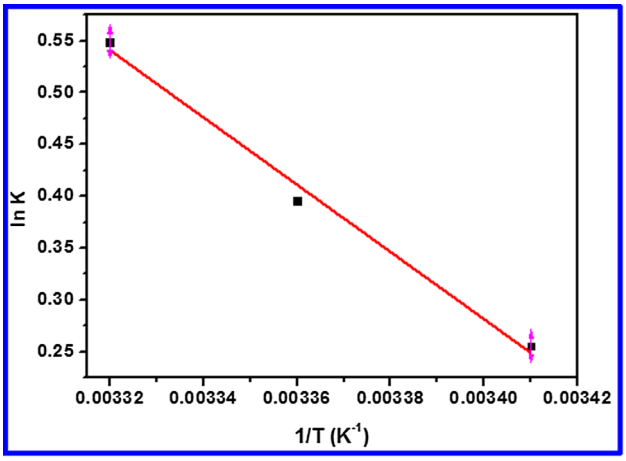

Fig. 3. Van't Hoff plots for HPFQ-human serum albumin interaction at different temperatures.

where F_0 and F are the fluorescence intensities in the absence and presence of the quencher HPFQ, respectively. According to Eq. (10), a linear plot of log $[(F_0 - F)/F]$ versus log [Q] will yield a slope equal to "n". This linear correlation (ESI Fig. S2) and slope value ("$n = 0.949$") adjacent to 1 indicate towards a single binding site for HPFQ with both plasma proteins. The binding constant (K_b) for HPFQ-HSA ($0.74 \times 10^5\,M^{-1}$) system indicates towards a moderate affinity for binding, when it gets compared to other protein-ligand interactions with greater binding constants (10^6 to $10^8\,M^{-1}$). It has been observed that, a weak binding interaction can cause loss of drug molecules from circulatory system and further decreasing its lifetime, whereas a robust binding affinity may reduce the concentration of liberated drug molecules in plasma and resists its diffusion at target sites. From this point of view, the moderate K_b value obtained here is imperative to understand the therapeutic efficiency and dynamic distribution of the bioactive fluorophore in plasma. Thus, it will indeed be intriguing to find out the forces that drives the protein-ligand interaction towards appreciable binding phenomena.

3.3. Quantifying the thermodynamic parameters of HPFQ-HSA association

Van't Hoff's plot has often been engaged to determine thermodynamic parameters for binding interactions and decipher the forces involved in it. There are believed to exist four main types of non-covalent interactions for ligand-protein binding: H-bonds, van der Waals forces, hydrophobic and electrostatic interactions [43]. Ross and Subramanian have provided us with the relation that exists between the signs and magnitudes of significant thermodynamic dimensions (ΔH and ΔS) with the governing forces dictating the protein-drug interaction process [44]: (1) $\Delta H < 0$ and $\Delta S < 0$ suggest domination of hydrogen bond and van der Waals force; (2) $\Delta H > 0$ and $\Delta S > 0$ indicates a dominant hydrophobic interaction and (3) if $\Delta H < 0$ and $\Delta S > 0$ imply that electrostatic interactions are dominant of all. For smaller temperature changes, the change in enthalpy (ΔH) of an interaction may be accepted as a constant. The ΔH and ΔS values of HPFQ-HSA interaction can be evaluated by employing Van't Hoff's equation:

$$\ln K = -\Delta H/RT + \Delta S/R \tag{11}$$

where K is equivalent to K_a, the effective association (or, quenching) constants at the same temperature and R is the universal gas constant. The tailored Stern-Volmer equation (Eq. (12)) is exploited to calculate K_a for the binding interaction between HPFQ and HSA [25]:

$$\boldsymbol{F_0/\Delta F = 1/f_a K_a [Q] + 1/f_a} \tag{12}$$

For HPFQ-HSA system, $\ln K$ exhibits a linear relationship with 1/T (Fig. 3), which in turn suggests for constant ΔH in the measured temperature range and can be calculated from the slope of the Van't Hoff plot, whereas the plot's intercept yields the value of ΔS. Furthermore, ΔG at various temperatures can be determined using the following equation:

$$\boldsymbol{\Delta G = \Delta H - T\Delta S = -RT\ln K} \tag{13}$$

The obtained ΔG value of the concerned quenching process turns out to be negative, which implies towards the quenching process to be spontaneous, leading to most favorable formation of HPFQ-HSA complex. Consequently, the above analysis also suggests towards ΔH and ΔS favoring spontaneity.

For HPFQ-HSA interaction, both ΔS and ΔH (Table 2) turn out to be positive, so the dimension $T\Delta S$ (in Eq. (13)) tends to grow larger than ΔH and results into a negative ΔG; which eventually indicates towards favorable and spontaneous binding process. Also, according to Ross and Subramanian, the positive ΔS and ΔH values suggest at existence of hydrophobic interaction between bioactive fluorophore and globular protein. The accessibility of the surface area of protein diminishes due to the binding of the drug to protein, which reciprocates by liberating solvent from the protein surface. Consequently, the system moves towards a favorable change in entropy, which is further manifested by a positive ΔS value. Thus, the dominance of hydrophobic interaction is established and it is also supported by the fact that several non-polar

Table 2
Quantification of thermodynamic parameters of HPFQ-HSA systems at different temperatures.

T (K)	K_a (L mol^{-1})	ΔH (kJ mol^{-1})	ΔG (J mol^{-1})	ΔS (J K^{-1} mol^{-1})	R[a]
293	1.038×10^5	26.978	−590.077	94.089	0.989
298	1.485×10^5		–1060.522		
303	1.949×10^6		–1531.967		

R[a] is the correlation factor for the modified Stern-Volmer plots.

groups in HPFQ moiety will proficiently interact with hydrophobic amino acid residues of HSA. Hence, hydrophobic interactions prove to be a key player in securing the bioactive molecule into protein scaffold, which further leads us towards investigation of favorable shelter for the bioactive probe inside the protein matrix.

3.4. Recognition of HPFQ binding site in human serum albumin

3.4.1. Evaluating the competitive binding assays in the presence of stereotypical site markers

The binding site of a drug inside a plasma protein provides us with crucial information about the bioactive molecule's restricted conformations which may be subjected to serious competition during occupancy of binding sites in HSA. For serving the purpose, displacement assays were carried out, to identify HPFQ binding site in HSA, using known probes with specific affinity towards a certain region of protein matrix. The crystal structure analysis of HSA protein designated two discrete binding sites, where majority of ligands bind with protein. According to Sudlow et al. [31], these principle sites are positioned in hydrophobic pockets present in subdomain IIA (Sudlow site I) and subdomain IIIA (Sudlow site II). For example, Warfarin prefers to bind at sudlow site I, whereas Ibuprofen preferentially occupies site II [45,46]. Thus, Warfarin and Ibuprofen may serve as site markers for respective binding sites of protein during comparative binding studies [47,48].

The hydrophobic interactions appear to play a dominant role in interaction between Warfarin and HSA. The benzyl ring of Warfarin interacts with Trp 214 to provide it stability inside the hydrophobic pocket of site I. Quenching of tryptophan fluorescence upon addition of War supports such observations. The other significant binding site, i.e., sudlow site II, that binds Ibuprofen, consists of a pocket at exterior site with two pertinent amino acid residues (Arg 410 and Tyr 411). This subdomain IIIA appears to demonstrate an elevated preference towards anions of long chain fatty acids.

Hence, competitive assays are performed where concentration of HPFQ is gradually increased to two separate systems of HSA in presence of two different prototypical site markers (Warfarin and Ibuprofen), where the ratio of concentration of protein and site markers are taken to be 1:1. Throughout these competitive binding studies, the novel ligand and corresponding site marker exhibit similar affinity for association, if they happen to occupy the identical binding site on the protein matrix. Thus, the change in intensity of the fluorescence spectra of such a system can reveal the degree of protein-ligand binding interaction.

In order to compare the authority of Warfarin and Ibuprofen on the binding of HPFQ to HSA, K_a of the therapeutic luminophore was calculated and analyzed in the absence and presence of stereotypical site markers. The fluorescence quenching data of HPFQ-HSA system yields the argument for the site specific binding of HPFQ. The binding constant of HPFQ with HSA, in presence of Warfarin is much smaller ($0.375 \pm 4.9 \times 10^5\,M^{-1}$) than that in its absence ($1.486 \pm 3.4\% \times 10^5\,M^{-1}$). But, the affinity in the presence of Ibuprofen is almost comparable ($1.065 \pm 2.6\% \times 10^5\,M^{-1}$) to the situation in the absence of Ibu (Table 3, Fig. 4). These findings expose the competition that exists between HPFQ and War due to their mutual affinity to bind at subdomain IIA or sudlow site I of HSA. Thus, the

Table 3
Affinity parameters derived from Site Competitive experiments at 298 K for HPFQ binding to HSA.

Site marker	K_a ($10^5\,M^{-1}$)	R[a]
Blank	1.486 ± 3.4%	0.9942
Ibuprofen	1.065 ± 2.6%	0.9869
Warfarin	0.375 ± 4.9%	0.9893

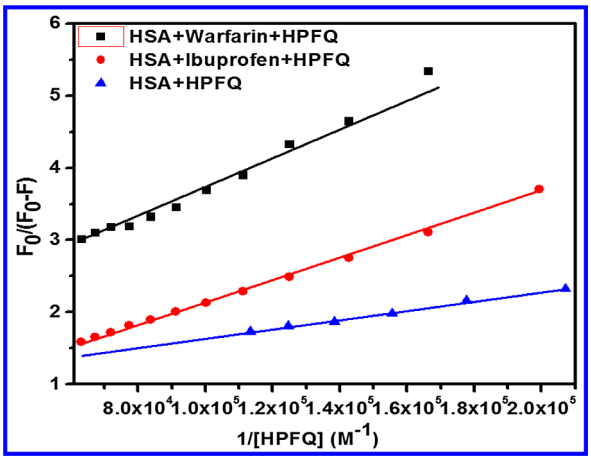

Fig. 4. Consequences of stereotypical site markers on binding of HPFQ to HSA in 10mMHepes buffer at 298 K; pH 7.4; where, [HSA]: [site marker] = 1:1.

guest anti-cancer luminophore is confirmed to be located in hydrophobic pockets of sudlow site I or subdomain IIA, which pronounces the probability of FRET occurring between donor HSA and acceptor HPFQ, as discussed in the relevant section.

3.4.2. Drug displacement investigation superintended by fluorescence anisotropy

The fluorescence anisotropy measurement engages in photoselective excitation of fluorescing probes by polarized light to yield polarized emission, because transition moments in absorption and emission have specific orientations within the fluorophore. These measurements offer us with a viewpoint about dynamics of protein conformation. Various factors such as shape of fluorophore, viscosity of solvent, flexibility of proteins control the anisotropic emission of molecule. Fluorescence anisotropy value gets enhanced when there is an increase of rigidity in surrounding of fluorophore. Consequently, the ease of rotation for fluorescing molecules in fluids calls for a lower anisotropic values, whereas different matrixes such as micelles and reverse micelles help to restrict the rotation and contribute to an increase in anisotropy value. Here, we have performed an experiment to have an idea of rotational restriction experienced by HPFQ molecule in protein matrix, by recording anisotropy value (r) of HPFQ with increasing concentration of the HSA protein (Fig. 5). The r value exhibits a striking increase, when HPFQ molecules move from aqueous bulk environment to protein matrix (0–0.24). Such an observation suggests towards restriction imposed on rotational diffusion of HPFQ by increasing the concentration of HSA, which in turn insists on binding of HPFQ within HSA structure.

Such measurement has also been exploited to identify the binding region of HPFQ inside HSA conformation, by increasing Warfarin and Ibuprofen separately after r value for HPFQ gets stabilized in HPFQ. After r value rides a plateau of 0.24 and levels off, introduction of War into HPFQ-HSA saturated system diminishes r value to 0.17. The momentous diminution in r value indicates at existing competition between Warfarin and HPFQ to conquer the identical position at sudlow site I of HSA. Whereas, introduction of Ibu in saturated HPFQ-HSA system does not seem to affect the r value of the system. Thus, the

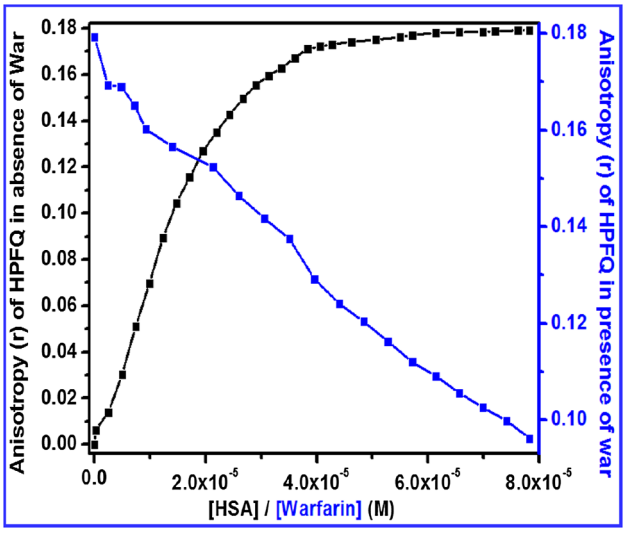

Fig. 5. Deviation in fluorescence anisotropy (*r*) of HPFQ with gradual increase in concentrations of HSA (-■-) and further upon achieving saturation with gradual increase in concentrations of site marker Warfarin (-■-). λ_{ex} = 328 nm for HPFQ and λ_{em} = 422 nm, T = 298 K for both readings. Average values of four independent experiments have been taken into consideration.

finding provides us with confirmation about HPFQ occupy Sudlow Site I of HSA, the same site where Warfarin also happens to bind with HSA.

3.5. Exhumation of the amino acid residues surrounding the therapeutic fluorophore and affirmation of binding pocket by in silico approach

Providing precise confirmation on binding of HPFQ at specific sites of HSA always proves to be a critical challenge, thanks to its over-abundance of binding sites and their inflated degree of malleability. In order to complement the spectroscopic results obtained *in vitro*, the site-specific interaction between the globular protein and the potential bioactive probe undergoes detailed investigation under amalgamated and coherent workflow of molecular docking and induced fit docking (IFD).

3.5.1. Visualization of the binding site by molecular docking of HPFQ with HSA

The binding approach and alignment of small bioactive molecules within HSA exhibits overwhelming influence on its conformational modulation and bioactivity under physiological condition [10,18]. The major binding domains in HSA are situated in hydrophobic pockets of subdomain II A and IIIA, which are also known as Sudlow site I and II respectively. The subdomain A consists of six α-helices while subdomain B possesses four α-helices. The computational approach aids us in decoding detailed binding interactions, providing us with a complete scenario of binding affinity and specificity [49,50].

In this context, the molecular docking studies were carried out using the crystal configuration of HSA (1AO6) to evaluate the binding site and modes of HPFQ inside globular protein, using a docking program named 'Glide'. 'Glide' explores the most favorable interaction between a receptor (generally, a protein) and an incoming ligand molecule by evaluating the different ligand alignments using OPLS force field.

The docking results for HPFQ-HSA system insist that HPFQ places itself within subdomain IIA while it interacts with Trp-214 in HSA via a π-π stacking. The binding site, where HPFQ warmly fits in, is also called 'Warfarin binding site' and it is constituted by a cavity (pocket) surrounded by several amino acid residues. In Fig. 6, these amino acid residues are indicated in green and they get involved in hydrophobic interaction with incoming ligand molecule. Besides hydrophobic interaction, electrostatic interactions and hydrogen bonding interactions also play key role in binding and stabilization of HPFQ in hydrophobic cavity of sudlow site I. The hydrophobic amino acid residues like Trp 214, Ala 215, Leu 219, Phe 223, Leu 234, Leu 238, Val 241, Ile 264 and Ala 291 helps to mobilize the anchoring of the bioactive ligand inside the protein cavity. Furthermore, involvement of Arg 257 and Lys 195 may result in blockage of esterase like catalytic activity of HSA in subdomain IIA. His 242 and Ser 269 are the polar amino acids, which underlies the HPFQ-HSA complex at site I. Thus, the docking results between HSA and HPFQ corroborates the experimental results which suggested involvement of hydrophobic interactions (from thermodynamic parameters) dominating the HPFQ-HSA interaction. The *in silico* results also agree with the site-specific experimental studies and confirm the location of HPFQ at sudlow site I, at 'War binding site' of HPFQ.

3.5.2. Investigation of surrounding amino acid residues at binding site by IFD study

The preliminary docking results prompted towards adaptation of more enlightening and suave method of Induced fit docking (IFD), which is capable of providing us with a vivid scenario of dynamic interaction between HPFQ and HSA. Schrodinger's IFD system provides a computational approach with more efficacy, to sample highly flexible binding sites in HSA. The reason is, here both the ligand and protein receptor are allowed to move freely. IFD capitulates Glide and refinement modules in 'Prime' program, which brings in adjustments in receptor structure; in order to closely resemble to conformations that facilitates binding shape and mode of the ligand. Such soft-docking attitude allows us to capture the dramatic modulation of side chain conformations, as well as the minor alterations induced in protein backbone structure. Such flexible adaptation of receptor system helps to eliminate the poorly scored binders (false negatives) obtained due to rigid receptor conformation' during docking study. This method assists us towards decoding the occupied site of the incoming small ligand molecule and its adopted pose at the site.

In context of HPFQ-HSA interaction, the IFD module indicates towards slight structural perturbation in the binding site (HSA), where HPFQ lies inside hydrophobic cavity acquiring its minimum energy conformation. HPFQ possesses a distorted chair conformation, with the non-functionalized E-ring lying close to Trp-214 residue. The average distance between the corresponding moieties turns out to be 2.67 nm (Fig. 7), which is in line with that (2.84 nm) obtained from the FRET calculation (discussed later). The IFD score of -1288.887 kcal mol^{-1} (ESI Fig. S3) indicates towards an optimal binding affinity between HPFQ and globular protein in aqueous buffer medium of pH 7.4. The IFD generated conformation suggests that the hydroxyl group of HPFQ forms a H-bond with Arg 257 (protein backbone), whereas the oxygen atom of furan moiety forms H-bond with Ly 195 (protein side-chain). 2D ligand interaction diagram points towards dominance of hydrophobic interaction because of major presence of hydrophobic amino acid residues (depicted as green balls) in immediate vicinity of bioactive fluorophore. The presence of positively charged residues like Lys-195, Arg-222, Arg-218 and Arg-257 are also noteworthy, for advanced designing of small drug molecules with enhanced HSA-drug interaction. Hence, hydrophobic, electrostatic and hydrogen bonding interactions play crucial parts in ensuring the habitation of ligand molecule at the occupied site inside the protein, which may further introduce minor conformational change in secondary structure of plasma protein.

3.6. HPFQ induced alteration in synergistic conformation of macromolecules

3.6.1. Deciphering the synchronous fluorescence spectra for HPFQ-HSA interaction

The excitation and emission monochromator are subjected to synchronized scanning in synchronous fluorescence spectroscopy, where a Δλ is fixed and maintained between them. This technique serves as an

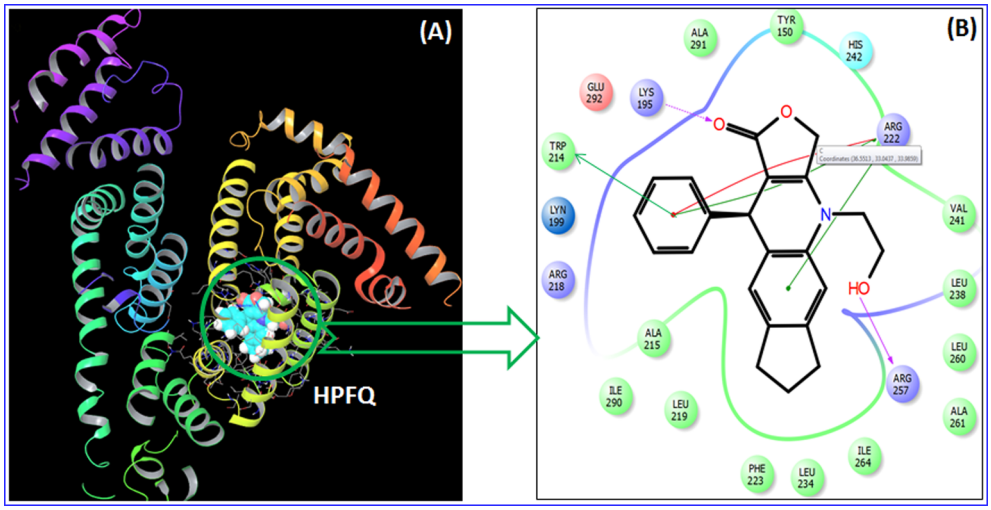

Fig. 6. (A) Conformation with minimum energy for HPFQ inside the binding pocket of sudlow site I of HSA (1A06); (B) Visualization of 2D-ligand interaction blueprint of amino acid residues situated adjacent to HPFQ at the binding site.

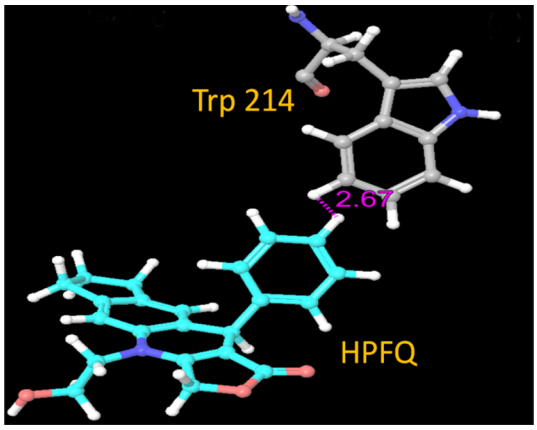

Fig. 7. Distance (expressed in nm) between Trp214 of HSA and the bound HPFQ in the docking pose comprising minimal energy, as illustrated by ball and stick model.

effective tool to measure fluorescence quenching and shift in emission maxima with respect to any variation in polarity around the fluorophore under controlled physiological conditions [51]. In synchronous fluorescence, stabilized $\Delta\lambda$ at 15 nm offers the characteristics of Tyr residue while $\Delta\lambda$ at 60 nm provides that of Trp residues in the plasma protein [52]. It has been observed that the fluorescence intensity of HSA diminished consistently, while being subjected to an increasing concentration of HPFQ, along with a significant blue shift (Fig. 8A) and is harmonious with the results of steady state fluorescence emission. This blue shift may suggest for minor conformational change in protein backbone. It may also indicate towards the location of amino acid residues in a more hydrophobic environment which implies that those residues will be less exposed to the solvent. Those observations were also supported by the values of thermodynamic parameters. However, for $\Delta\lambda$ = 15 nm, no shift in emission maxima was observed (Fig. 8B), which indicates that the interaction between the therapeutic luminophore and HSA does not perturb the regional conformation around Tyrosine residue.

From the Fig. 10, it is evident that the quenching in protein emission for $\Delta\lambda$ = 60 nm (62.3%) is greater than that for $\Delta\lambda$ = 15 nm. Such observation endorses the fact that HPFQ inhabits at site in Sudlow site I, where Trp214 (sole Tryptophan residue in HSA), is situated. Contrarily, quenching of Tyrosine residues (when $\Delta\lambda$ = 15 nm) is found to be 41.3%, in the presence of ligand, which is much lesser compared to that for Trp residue. While Trp214 is positioned at Sudlow site I and Tyr263 inhabits at subdomain IIIA (site II), it can be resolved that the binding

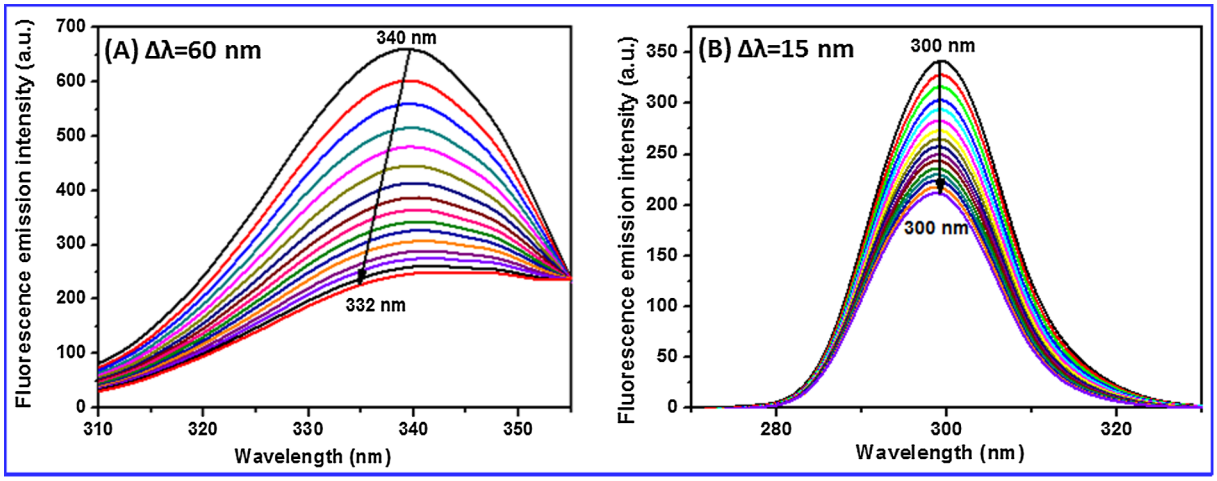

Fig. 8. Illustration of Synchronous fluorescence spectra for HSA in the presence of various concentrations of HPFQ: [HSA] = 1 μM; [HPFQ] = 0–25.5 μM; pH 7.0; T = 298 K (A) $\Delta\lambda$ = 60 nm; (B) $\Delta\lambda$ = 15 nm.

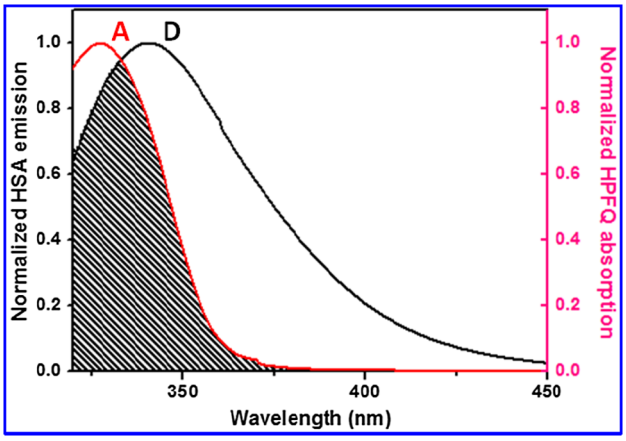

Fig. 9. Overlap of spectral lines for absorption of HPFQ (A, Acceptor) and fluorescence of HSA (D, Donor), where [HSA] = [HPFQ] = 1 μM.

site of HPFQ is accessible by both Trp and Tyr residues of HSA. The consequences of the above experiment establishes that HPFQ binds in the hydrophobic cavity of Sudlow site I (subdomain IIA) of HSA, which agrees impressively with steady state fluorescence quenching studies, competitive binding assays and *in silico* docking calculations.

3.6.2. Impact on conformation of HSA by HPFQ as governed by circular dichroism

Binding of a bioactive ligand to HSA may induce structural and conformational modification of the receptor molecule. If the ligand brings in a major conformational alteration in protein structure, that may perturb the biochemical activity of the protein. The preservation of active sites in protein structure forms its cardinal function, which suggests that minimal conformation change in protein structure is highly appreciated. The transport mechanism of a bioactive probe depends on the conformational flexibility of the receptor to promote the interaction with the probe molecule.

Circular Dichroism (CD) spectroscopy is a very responsive tool to investigate the modulation in secondary structure and conformation of proteins, induced by incoming ligands. In this context, to examine the modulation (if any) in secondary structure of receptor protein upon habilitation of the HPFQ molecule at physiological pH with different concentration, CD is performed in far UV region of 200–260 nm [26].

The CD spectra of native HSA, in absence of HPFQ, exhibits negative absorption bands with dual maxima at 222 nm (n-π^*) and 208 nm (π-π^*), according to typical α-helical characteristic of protein [53,54]. On gradual increment of HPFQ concentration, of two bands at 208 and 222 nm exhibit a decrement in negative ellipticity (ESI Fig. S4), which suggests an increase in negative cotton effect and subsequently insists towards slight conformational change in secondary protein structure.

The quantitative analysis of α-helical content of exhibits a reduction in its quantity upon increasing amount of HPFQ within HSA matrix. The α-helical content of native protein appears to be 70%, whereas that declines to 60% for HPFQ-HSA complex. Such small diminution of α-helix induces a minor conformational change in native HSA structure. Such minor change may result in atomic shuffling of amino acid residues in HSA to a certain extent and partial destruction in H-bonding interaction, which makes the polypeptide chain slightly more ductile to accommodate HPFQ inside the protein matrix. Thus, a slender loosening of HSA polypeptide backbone helps it to adopt a more accessible conformation to fit HPFQ in its scaffold. Such minor conformational change in secondary structure of HSA may not destruct its inherent activity but may somehow affect the rotamerisation of Trp-214 residue in protein backbone.

3.7. Rationale for the dynamic behavior of HPFQ-HSA association

The probable binding location of therapeutic luminophore HPFQ in subdomain IIA (sudlow site I) of globular protein matrix lies in the hydrophobic region, where Trp 214 residue also happens to exist in close proximity. Such relative positioning of therapeutic chromophore and protein fluorophore increases the probability of FRET between HSA emission and HPFQ absorption. FRET is often regarded as a "spectroscopic ruler" as, it can assist to unveil the distance between donor and acceptor residues in an interactive system [55]. Generally, FRET takes place when emission of a donor molecule exhibits significant overlap with absorption of an acceptor molecule, while the distance between them for effective energy transfer lies in the range of 2–8 nm [56]. So, the FRET process generally depends on four major conditions and they are: (i) molar absorptivity co-efficient and quantum yield of donor (D), (ii) overlap integral between the absorption and emission spectrum of acceptor and donor respectively, (iii) the correlative orientation of the transition dipoles for donor (D) and acceptor (A), and (iv) the distance (r_0) between D and A [55].

The normalized emission spectra of HSA in buffer solution exhibits a substantial overlap with normalized absorption spectra of HPFQ, as shown in Fig. 9. The following Förster's theory can be exploited to determine the efficacy of energy transfer (E) and the distance (*r)* between donor and acceptor by [25]:

$$E = 1 - \frac{F}{F_0} = \frac{R_0^6}{R_0^6 + r} \tag{14}$$

where, E denotes efficacy of energy transfer between D and A, *r* is distance between them.

The critical distance, R_0,at which the transfer efficiency equals 50% can be measured by the following equation [25]:

$$R_0^6 = 8.8 \times 10^{-25}[\kappa^2 n^{-4} \varphi_D J] \tag{15}$$

where κ^2 is the spatial orientation factor related to the geometry of D and A dipoles, and also generally found to be equal to 2/3 for random orientation as in fluid solution, n is refractive index of the medium, φ_D is fluorescence quantum yield of donor. The quantity Jprovides the degree of spectral overlap integral between donor emission and acceptor excitation, which is given by [25]:

$$J = \frac{\int_0^\infty F(\lambda)\varepsilon(\lambda)\lambda^4 d\lambda}{\int_0^\infty F(\lambda) d\lambda} \tag{16}$$

where $F_d(\lambda)$ is the normalized donor emission spectrum in the range from λ to λ + Δλ and $\varepsilon_a(\lambda)$ is the molar absorption coefficient of the acceptor at wavelength λ. For the present HPFQ-HSA interaction, we use the following values: $\kappa^2 = 2/3$, $n = 1.33$, $\varphi_D = 0.118$, ε_a for HPFQ = $1.818 \times 10^4\,M^{-1}\,cm^{-1}$ at 422 nm. Using the related values and experimental data in appropriate above equations, we evaluate the following quantities: $J(\lambda) = 2.41 \times 10^{14}\,M^{-1}\,cm^{-1}$, $R_0 = 2.84$ nm, $r = 2.18$ nm, and E = 0.854. The results evidently agrees with Forster's theory, as value of *r* exists within the range of 2–8 nm, i.e., *r lies in between* 0.5 R_0 *and* 1.5 R_0, which means that there exists a transfer of energy between HPFQ and HSA due to their close proximity (also supported by steady state emission and TRF measurements). The distance (2.84 nm) between bound HPFQ and Trp-214 obtained from FRET also lies in good accordance with the one derived from IFD calculation (Fig. 7). Such dynamic interaction between carrier protein and the probe helps to bring in a modulation in excited state of intrinsic fluorophore in HSA, which may lead to inter-conversion of the conformers that exists for it.

3.8. Disclosure of excited-state dynamics and bestowing a vibrant picture for specific control over rotamerisation of Trp 214 in HSA

Time resolve fluorescence techniques are often exploited as a sensitive tool for inspecting the alteration in local environment around a fluorophore. This method subsequently contributes towards assimilation of probe-protein interactions. Here, TRF experiment has been carried out to elucidate the quenching mechanism of Trp intrinsic fluorescence, while being in and out of contact with HPFQ [12]. The native HSA in buffer exhibits tri-exponential decay of its lifetime, due to existence of different rotamers of sole Tryptophan residue (Trp-214) [57–59]. The decay profile of HSA, in presence of HPFQ, also reveals existence of tri-exponential fitting simultaneously.

The three rotamers of tryptophan with lifetimes of 1.1 ns (τ_1), 3.96 (τ_2) and 7.32 (τ_3) are referred to as conformer I, II and III respectively. The inconsistency in lifetime and relative contribution of three rotamers virtually indicates towards their discrepancy in relative exposure to surrounding microenvironment. The larger lifetime component is often referred to as 'free rotamer' and suggests for the larger exposure of the residue to the aqueous microenvironment. Whereas, the shortest and the intermediate components reflect about the rigidity of Tryptophan microenvironment and lowering of their values indicates towards the vulnerability towards less polar environment and their deep burial inside the amino acid residues, away from bulk aqueous media.

When the globular protein is exposed towards increasing concentration of HPFQ, the bioactive ligand casts different spell over the conformers. τ_3 seems to remain unaffected throughout the experimental concentration range suggesting that HPFQ probably likes to ignore any kind of interaction with conformer III. τ_1, having the shortest lifetime, also marginally decreases from 1.50 to 1.39 ns while that of conformer II, τ_2 demonstrates appreciable reduction of 5.04–3.99 ns which emphasizes for greater interaction between HPFQ and intermediate conformer of Trp residue in HSA.

The τ_f value of HSA decreases remarkably, in presence of HPFQ. The plot of τ_0/τ (ESI Fig. S5) yields a biphasic curve (or, two straight lines with different slopes per say) with respect to the concentration of HPFQ, which suggests towards simultaneous action of dynamic and static quenching mechanism between HPFQ and HSA. Simultaneously, the Trp fluorescence lifetime decay profiles, in presence of HPFQ, also indicates towards manifestation of dynamic quenching mechanism, which may evolve from FRET occurring between bioactive probe and the receptor protein. Such collisional process operated between HPFQ and HSA may instigate minor conformational change in secondary structure of carrier protein.

We also observed another interesting trend regarding the ardent modulation in relative percentage contribution of three rotamers in HSA, upon increment in concentration of HPFQ. The percentage contribution declines thoroughly for conformer II from 46.30 to 30.30%, whereas the reverse situation arises for conformer I when percentage contribution starts escalating from 26.5% to 43.1% value (Fig. 11) (Table 4). The contribution of conformer III remains more or less indifferent throughout the experiment. Thus, in the context of concentration dependent HPFQ binding to HSA, the switching in the relative percentage contribution and radiative lifetime decays of the three rotamers indicates towards the fact that HPFQ instigates specific perturbations in the Trp-214 neighborhood. HPFQ specifically prefers to interact with the rotamer of intermediate lifetime and causes the quenching in intrinsic fluorescence of HPFQ. The blue shift observed in emission spectra can also be corroborated with the interaction of HPFQ with the rotamer II, which sits deeply buried inside the matrix. This nature of variation also verify that HPFQ does exhibit a scrupulous control over the rotamerisation of Trp-214, which may be either due to the minor conformational modification in the secondary structure of the transport protein, or, by the direct interaction between HPFQ and Trp-214 or both.

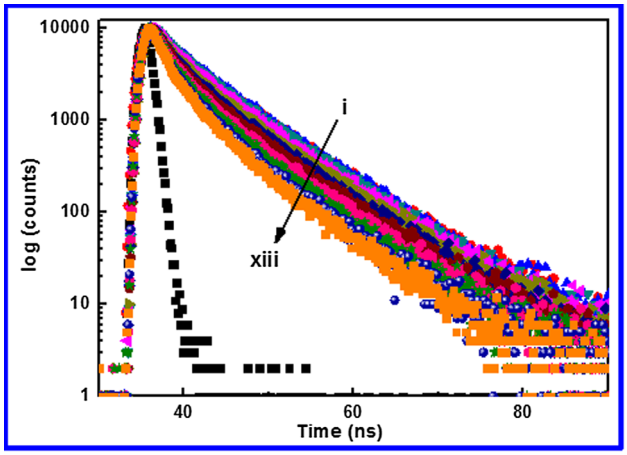

Fig. 10. The decay profile corresponding to time-resolved fluorescence for HSA-HPFQ systems at 298 K. [HPFQ] = 0–9.61 μM (i–xiii).

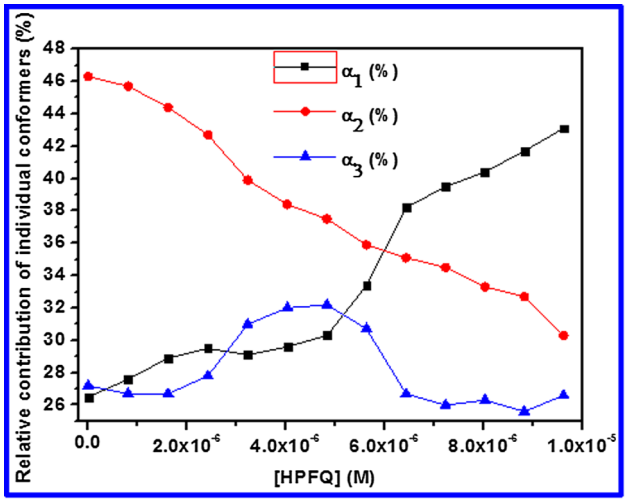

Fig. 11. Relative Percentage contribution of three structural rotamers in native HSA with increasing HPFQ at 298 K. (λ_{ex} = 280 nm, λ_{em} = 340 nm).

Table 4
Parameters related to fluorescence lifetime decay of HSA conformers in the presence of HPFQ.

[HPFQ] (μM)	τ_1 (ns)	τ_2 (ns)	τ_3 (ns)	α_1 (%)	α_2 (%)	α_3 (%)	χ^2	τ_f (ns)
0	1.5	5.04	7.95	26.5	46.3	27.2	1.03	4.89342
8.08E−07	1.36	5.01	7.38	27.6	45.7	26.7	1.145	4.63539
1.61E−06	1.48	4.6	7.89	28.9	44.4	26.7	1.14	4.57675
2.42E−06	1.08	4.7	7.4	29.5	42.7	27.8	1.08	4.3827
3.22E−06	1.02	3.99	7.97	29.1	39.9	31	1.11	4.35953
4.03E−06	1.16	3.39	7.59	29.6	38.4	32	1.32	4.07392
4.83E−06	1.2	3.44	7.1	30.3	37.5	32.2	1.25	3.9398
5.63E−06	1.13	3.79	7.09	33.4	35.9	30.7	1.07	3.91466
6.43E−06	1.17	4.03	7.44	38.2	35.1	26.7	1.17	3.84795
7.23E−06	1.07	3.98	7.69	39.5	34.5	26	1.21	3.79515
8.02E−06	1.58	3.57	7.41	40.4	33.3	26.3	1.23	3.77596
8.82E−06	1.53	3.75	7.37	41.7	32.7	25.6	1.05	3.75098
9.61E−06	1.31	3.99	7.26	43.1	30.3	26.6	0.927	3.70474

3.9. pH sensitive behavior of microconformer of Trp 214 in presence of HPFQ

Variation in pH is believed to bring about conformational alteration in native structure of HSA protein. According to TRF studies performed in case of native HSA in aqueous buffer solution at 25 °C (298 K), there

are several structural configurations present in HSA structure. HSA acquires E (extended form) in pH 2 and 3. In pH range 4–10, it exhibits three different arrangements: migrating (F), normal (N) and basic (B) forms, which do not show much modulation in structural formalities [59,60]. At the extreme basic pH of 11–12, HSA procures the aged form (A) in its structural modulation. The lifetime and pre-exponential values of three lifetime components in Trp 214 plausibly depends upon the extent of interaction taking place between Trp residues and their surrounding microenvironment [9]. In this context, the three conformers of Trp 214 acquires specific orientation within HSA native structure, under different configurations of carrier protein. The previous lifetime studies of HSA reveal that, the two shorter lifetimes are more sensitive towards hydrophobic interaction, whereas the one with the largest lifetime corroborates higher sensitivity towards hydrophilic neighborhood [59]. This finding suggests relative exposure of these rotamers towards solvent molecules under different conformational modulation of HSA, although they all reside at sudlow site I and confirms their comparative measure of interaction with microenvironments of different polarity.

Such results agrees well with our experimental findings and clearly indicates that the bioactive probe HPFQ move towards relatively non-polar region and can voluntarily modulate the lifetime and population of conformer I and II; while subsequently showing indifferent attitude towards conformer III, who is believed to be inclined towards hydrophilic interactions. Moreover, we have chosen three such pH (Fig. 12) that they represent three different configuration of native protein structure (F, N and B forms show similar configuration and prompted us to select single pH in this range). The pH based quenching study performed in presence of HSA and increasing concentrations of HPFQ suggests that the extent of quenching in intrinsic fluorescence of Trp 214 increases while we move from acidic pH to physiological pH and then decreases again for basic pH. The interaction of HSA-HPFQ system is found to be highest in pH 7, intermediate in pH 3 and lowest in pH 11. This revelation suggests that the rotamer II orient itself in such a manner that it is more exposed towards hydrophobic interaction in normal form (N) of HSA. The declination in quenching constants with acidic and basic pH indicates that the structural modification in HSA protein at different pH modulates the orientation of rotamer II in such a manner that it gradually distances itself from such interactions, which in turn resists any kind of dynamic interaction between probes invading at surrounding environment and the rotamer II of HSA. The previous pH dependent lifetime measurements of Trp rotamer lifetime also suggested towards a more or less constant percentage contribution towards intrinsic emission of HSA, which makes it an ideal candidate to be affected by incoming ligand, if we aim towards an effective binding interaction between particular Trp 214 residue and the non-polar bioactive probe.

This pH dependent binding study helps us to decipher, how the rotamer II alters its orientation with structural changes in HSA and how that impacts its interaction with any change in surrounding microenvironment.

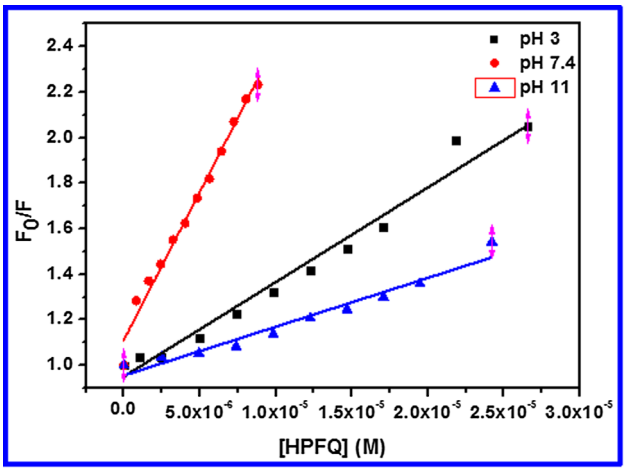

Fig. 12. Modified Stern-Volmer plot for HPFQ-HSA interaction at different pH, at 298 K. (λ_{ex} = 295 nm; λ_{em} = 340 nm).

4. Conclusion

An insight into the molecular mechanism behind the interaction between human serum albumin and the anti-proliferative luminophore HPFQ molecule has proved to be essential for effective transport of the drug to active sites inside the human body. In this context, the comprehensive *in vitro* spectroscopic study accompanied by *in silico* molecular docking, has been utilized to decipher the binding interaction between HSA and a therapeutic fluorophore HPFQ and the conformational flexibility that HPFQ introduces into sudlow site I (subdomain IIA) of carrier protein matrix. The appreciable binding strength of HSA makes it an excellent candidate for transport of the therapeutic luminophore inside human biological system. The quenching of intrinsic fluorescence of HSA undergoes simultaneous static and dynamic mechanism, in presence of HPFQ, as demonstrated by steady state quenching experiments and TRF measurements. FRET is considered to play a pivotal role in bringing such dynamic component into the protein-drug interaction; arising due to close proximity (2.67 nm) of HPFQ and Trp 214 of HSA. The dynamic interaction between HPFQ and HSA may also be subjected to the fact, how HPFQ regulates the population of different rotamers of Trp 214, as determined from TRF studies and its favorable interaction with conformer II exhibits the specific influence that HPFQ possesses over amino acids at its surroundings inside the binding domain of transport protein. The minimal perturbation into secondary structure of protein, induced by HPFQ, has been confirmed by synchronous fluorescence and CD spectroscopic explorations. The distinct molecular docking studies accompanied by steady state emission, drug displacement assay, fluorescence anisotropy, synchronous fluorescence and TRF measurements confirm that HSA embraces the binding of HPFQ into the hydrophobic cavity of sudlow site I (subdomain IIA) in HSA. The IFD study brings evidence of conformational flexibility exhibited by HSA into adapting HPFQ, whereas the binding is simultaneously anchored by hydrophobic, electrostatic and hydrogen bonding interactions. This vigilant inspection into binding of HPFQ at sudlow site I of HSA is destined to provide valuable information for judicious exploitation and modified design of therapeutics from azapodophyllotoxin class of compounds with domain specific binding to HSA. The study also helps to raise the curtain on mechanistic details of azapodophyllotoxin class of therapeutic fluorophores on regulatory attitude towards Trp rotamers in HSA. The consolidated research herein insist that HSA exhibits a magnanimous attitude towards adapting HPFQ by introducing conformational flexibility at binding site of sudlow site I, resulting in an effective binding and invigorates deploying of HSA-based transport and distribution system for such bioactive luminophores.

Acknowledgement

The authors are indebtedly grateful to Department of Chemistry, VNIT, Nagpur for providing the necessary facilities. The authors would like to convey their gratitude to Ms. Anuja Singh for her kind help. Research reported in this publication was partly supported by an Institutional Development Award (IDeA) from the National Institute of General Medical Sciences of the National Institutes of Health under grant number P20 GM103475-14. The content is solely the responsibility of the authors and does not necessarily represent the official views of the National Institutes of Health. The authors also thank and appreciate the constructive comments from the anonymous respected Reviewers to enrich the quality of the manuscript.

Appendix A. Supplementary material

Supplementary data to this article can be found online at https://doi.org/10.1016/j.bioorg.2018.11.015.

References

[1] G. Fanali, A. di Masi, V. Trezza, M. Marino, M. Fasano, Human serum albumin: from bench to bedside, Mol. Aspects Med. 33 (2012) 209–290, https://doi.org/10.1016/J.MAM.2011.12.002.

[2] U. Kragh-Hansen, Structure and ligand binding properties of human serum albumin, Dan. Med. Bull. 37 (1990) 57–84 (accessed May 27, 2018), http://www.ncbi.nlm.nih.gov/pubmed/2155760.

[3] S. Sugio, A. Kashima, S. Mochizuki, M. Noda, K. Kobayashi, Crystal structure of human serum albumin at 2.5 Å resolution, Protein Eng. Des. Sel. 12 (1999) 439–446, https://doi.org/10.1093/protein/12.6.439.

[4] M.Z. Kabir, W.-V. Tee, S.B. Mohamad, Z. Alias, S. Tayyab, Interaction of an anticancer drug, gefitinib with human serum albumin: insights from fluorescence spectroscopy and computational modeling analysis, RSC Adv. 6 (2016) 91756–91767, https://doi.org/10.1039/C6RA12019A.

[5] R. Thakur, A. Das, V. Sharma, C. Adhikari, K. Sundar Ghosh, A. Chakraborty, Interaction of different prototropic species of an anticancer drug Ellipticine with HSA and IgG proteins: multispectroscopic and molecular modeling studies, (n.d.). www.rsc.org/pccp (accessed May 28, 2018).

[6] F. Shen, Y.-X. Liu, S.-M. Li, C.-K. Jiang, B.-F. Wang, Y.-H. Xiong, Z.-W. Mao, X.-Y. Le, Synthesis, crystal structures, molecular docking and in vitro cytotoxicity studies of two new copper (i) complexes: special emphasis on their binding to HSA, New J. Chem. 41 (2017) 12429–12441, https://doi.org/10.1039/C7NJ02351K.

[7] X.M. He, D.C. Carter, Atomic structure and chemistry of human serum albumin, Nature 358 (1992) 209–215, https://doi.org/10.1038/358209a0.

[8] W. Qiu, L. Zhang, Oghaghare Okobiah, A. Yi Yang, D. Lijuan Wang, A.H. Zewail Zhong, Ultrafast solvation dynamics of human serum albumin: correlations with conformational transitions and site-selected recognition, J. Phys. Chem. B 110 (2006) 10540–10549, https://doi.org/10.1021/JP055989W.

[9] A. Del Giudice, C. Dicko, L. Galantini, N.V. Pavel, Time-dependent pH scanning of the acid-induced unfolding of human serum albumin reveals stabilization of the native form by palmitic acid binding, J. Phys. Chem. B 121 (2017) 4388–4399, https://doi.org/10.1021/acs.jpcb.7b01342.

[10] B. Meloun, L. Morávek, V. Kostka, Complete amino acid sequence of human serum albumin, FEBS Lett. 58 (1975) 134–137, https://doi.org/10.1016/0014-5793(75)80242-0.

[11] B. Sengupta, A. Acharyya, P. Sen, Elucidation of the local dynamics of domain-III of human serum albumin over the ps–μs time regime using a new fluorescent label, Phys. Chem. Chem. Phys. 18 (2016) 28548–28555, https://doi.org/10.1039/C6CP05743H.

[12] M. Nairat, A. Konar, M. Kaniecki, V.V. Lozovoy, M. Dantus, Investigating the role of human serum albumin protein pocket on the excited state dynamics of indocyanine green using shaped femtosecond laser pulses, Phys. Chem. Chem. Phys. 5872 (2015) 5872–5877, https://doi.org/10.1039/c4cp04984e.

[13] B. Sengupta, P.K. Sengupta, The interaction of quercetin with human serum albumin: a fluorescence spectroscopic study, Biochem. Biophys. Res. Commun. 299 (2002) 400–403, https://doi.org/10.1016/S0006-291X(02)02667-0.

[14] H. Kumar, V. Devaraji, R. Joshi, S. Wankar, S.K. Ghosh, A Chalcone-based potential therapeutic small molecule that binds to subdomain IIA in HSA precisely controls the rotamerization of Trp-214, ACS Omega 3 (2018) 10114–10128, https://doi.org/10.1021/acsomega.8b01079.

[15] J.W. Petrich, M.C. Chang, D.B. McDonald, G.R. Fleming, On the origin of non-exponential fluorescence decay in tryptophan and its derivatives, J. Am. Chem. Soc. 105 (1983) 3824–3832, https://doi.org/10.1021/ja00350a014.

[16] A.G. Szabo, D.M. Rayner, Fluorescence decay of tryptophan conformers in aqueous solution, J. Am. Chem. Soc. 102 (1980) 554–563, https://doi.org/10.1021/ja00522a020.

[17] P. Silvi Antonini, W. Hillen, N. Ettner, W. Hinrichs, P. Fantucci, S.M. Doglia, J.A. Bousquet, M. Chabbert, Molecular mechanics analysis of Tet repressor TRP-43 fluorescence, Biophys. J. 72 (1997) 1800–1811, https://doi.org/10.1016/S0006-3495(97)78826-X.

[18] O.K. Abou-zied, O.I.K. Al-Shihi, Characterization of subdomain IIA binding site of human serum albumin in its native, unfolded, and refolded states using small molecular probes, J. Am. Chem. Soc. 130 (2008) 10793–10801, https://doi.org/10.1021/ja8031289.

[19] A. Kumar, V. Kumar, A.E. Alegria, S.V. Malhotra, Synthetic and application perspectives of azapodophyllotoxins: alternative scaffolds of podophyllotoxin, Curr. Med. Chem. 18 (2011) 3853–3870.

[20] A. Kumar, V. Kumar, A.E. Alegria, S.V. Malhotra, N-hydroxyethyl-4-aza-didehydropodophyllotoxin derivatives as potential antitumor agents, Eur. J. Pharm. Sci. 44 (2011) 21–26, https://doi.org/10.1016/j.ejps.2011.04.013.

[21] S.V.M. Ajay Kumar, Vineet Kumar, Antonio E. Alegria, N-Hydroxyethyl-4-aza-didehydropodophyllotoxin derivatives as potential antitumor agents, Eur. J. Pharm. Sci. 44 (2011) 21–26, https://doi.org/10.1016/j.ejps.2011.04.013.

[22] A. Kumar, A.E. Alegria, Synthesis of novel functionalized 4-Aza-2,3-didehydropodophyllotoxin derivatives with potential antitumor activity, J. Heterocycl. Chem. 47 (2010) 1275–1282, https://doi.org/10.1002/jhet.467.

[23] S.K. Ghosh, R. Joshi, S. Mukherjee, A. Kumar, A. Singh, M. Concepcion-Santana, Unusual photophysics of anticancer azapodophyllotoxin: the collective effect of discrete H-bond motif spills the beans, J. Photochem. Photobiol. A Chem. 349 (2017) 49–62, https://doi.org/10.1016/j.jphotochem.2017.08.069.

[24] S. Biswas, P.K. Chowdhury, Correlated and anticorrelated domain movement of human serum albumin: a peek into the complexity of the crowded milieu, J. Phys. Chem. B 120 (2016) 4897–4911, https://doi.org/10.1021/acs.jpcb.6b01671.

[25] J.R. Lakowicz, Principles of Fluorescence Spectroscopy, Springer, 2007.

[26] F.S. Graciani, V.F. Ximenes, Investigation of human albumin-induced circular dichroism in dansylglycine, PLoS One 8 (2013) e76849, https://doi.org/10.1371/journal.pone.0076849.

[27] Schrodinger Inc, LigPrep User Manual LigPrep 2.3 User Manual LigPrep User Manual, (n.d.). https://isp.ncifcrf.gov/files/isp/uploads/2010/07/lp23_user_manual.pdf (accessed May 28, 2018).

[28] T.A. Halgren, R.B. Murphy, R.A. Friesner, H.S. Beard, L.L. Frye, A.W. Thomas Pollard, J.L. Banks, Glide: a new approach for rapid, accurate docking and scoring. 2. Enrichment factors in database, Screening (2004), https://doi.org/10.1021/JM030644S.

[29] R.A. Friesner, R.B. Murphy, M.P. Repasky, L.L. Frye, J.R. Greenwood, T.A. Halgren, P.C. Sanschagrin, D.T. Mainz, Extra precision glide: docking and scoring incorporating a model of hydrophobic enclosure for protein−ligand complexes, J. Med. Chem. 49 (2006) 6177–6196, https://doi.org/10.1021/jm051256o.

[30] P. Ghosh, J. Patwari, S. Dasgupta, Complexation with human serum albumin facilitates sustained release of morin from polylactic-Co-glycolic acid nanoparticles, J. Phys. Chem. B 121 (2017) 1758–1770, https://doi.org/10.1021/acs.jpcb.6b08559.

[31] G. Sudlow, D.J. Birkett, D.N. Wade, Further characterization of specific drug binding sites on human serum albumin, Mol. Pharmacol. 12 (1976).

[32] X. Ma, J. Yan, K. Xu, L. Guo, H. Li, Binding mechanism of trans-N-caffeoyltyramine and human serum albumin: investigation by multi-spectroscopy and docking simulation, Bioorg. Chem. 66 (2016) 102–110, https://doi.org/10.1016/J.BIOORG.2016.04.002.

[33] O. Dömötör, T. Tuccinardi, D. Karcz, M. Walsh, B.S. Creaven, É.A. Enyedy, Interaction of anticancer reduced Schiff base coumarin derivatives with human serum albumin investigated by fluorescence quenching and molecular modeling, Bioorg. Chem. 52 (2014) 16–23, https://doi.org/10.1016/J.BIOORG.2013.10.003.

[34] A. Ali, M. Asif, P. Alam, M. Jane Alam, M. Asif Sherwani, R. Hasan Khan, S. Ahmad, Shamsuzzaman, DFT/B3LYP calculations, in vitro cytotoxicity and antioxidant activities of steroidal pyrimidines and their interaction with HSA using molecular docking and multispectroscopic techniques, Bioorg. Chem. 73 (2017) 83–99, https://doi.org/10.1016/J.BIOORG.2017.06.001.

[35] D. Sousa-Pereira, O.A. Chaves, C.M. dos Reis, M.C.C. de Oliveira, C.M.R. Sant'Anna, J.C. Netto-Ferreira, A. Echevarria, Synthesis and biological evaluation of N-aryl- 2-phenyl-hydrazinecarbothioamides: experimental and theoretical analysis on tyrosinase inhibition and interaction with HSA, Bioorg. Chem. 81 (2018) 79–87, https://doi.org/10.1016/J.BIOORG.2018.07.035.

[36] A. Mallick, B. Haldar, S. Maiti, S.C. Bera, N. Chattopadhyay, Photophysical study of 3-Acetyl-4-oxo-6,7-dihydro-12 *H* -indolo[2,3-*a*]quinolizine in biomimetic reverse micellar nanocavities: a spectroscopic approach, J. Phys. Chem. B 109 (2005) 14675–14682, https://doi.org/10.1021/jp050511d.

[37] A. Samanta, B.K. Paul, N. Guchhait, Studies of bio-mimetic medium of ionic and non-ionic micelles by a simple charge transfer fluorescence probe N, N-dimethylaminonapthyl-(acrylo)-nitrile, spectrochim, Acta Part A Mol. Biomol. Spectrosc. 78 (2011) 1525–1534, https://doi.org/10.1016/j.saa.2011.01.044.

[38] S.W. Chen, S. Drakulic, E. Deas, M. Ouberai, F.A. Aprile, R. Arranz, S. Ness, C. Roodveldt, T. Guilliams, E.J. De-Genst, D. Klenerman, N.W. Wood, T.P.J. Knowles, C. Alfonso, G. Rivas, A.Y. Abramov, J.M. Valpuesta, C.M. Dobson, N. Cremades, Structural characterization of toxic oligomers that are kinetically trapped during α-synuclein fibril formation, Proc. Natl. Acad. Sci. 112 (2015) E1994–E2003, https://doi.org/10.1073/pnas.1421204112.

[39] M. Jadhao, P. Ahirkar, H. Kumar, R. Joshi, O.R. Meitei, S.K. Ghosh, Surfactant induced aggregation–disaggregation of photodynamic active chlorin e6 and its relevant interaction with DNA alkylating quinone in a biomimic micellar microenvironment, RSC Adv. 5 (2015) 81449–81460, https://doi.org/10.1039/C5RA16181A.

[40] N.C. Maiti, M.M.G. Krishna, P.J. Britto, N. Periasamy, Fluorescence dynamics of dye probes in micelles, J. Phys. Chem. B 101 (1997) 11051–11060, https://doi.org/10.1021/jp9723123.

[41] M. Jadhao, S. Mukherjee, R. Joshi, H. Kumar, S.K. Ghosh, RSC Advances Aggregation – disaggregation pattern of photodynamically active ZnPcS 4 and its interaction compactness and central metal ion †, RSC Adv. 6 (2016) 77161–77173, https://doi.org/10.1039/C6RA13151D.

[42] J. Keizer, Nonlinear fluorescence quenching and the origin of positive curvature in Stern-Volmer plots, J. Am. Chem. Soc. 105 (1983) 1494–1498, https://doi.org/10.1021/ja00344a013.

[43] B.K. Paul, N. Ghosh, S. Mukherjee, Interplay of multiple interaction forces: binding of norfloxacin to human serum albumin, J. Phys. Chem. B 119 (2015) 13093–13102, https://doi.org/10.1021/acs.jpcb.5b08147.

[44] P.D. Ross, S. Subramanian, Thermodynamics of protein association reactions: forces contributing to stability, Biochemistry 20 (1981) 3096–3102, https://doi.org/10.1021/bi00514a017.

[45] P.B. Kandagal, S. Ashoka, J. Seetharamappa, S.M.T. Shaikh, Y. Jadegoud, O.B. Ijare, Study of the interaction of an anticancer drug with human and bovine serum albumin: spectroscopic approach, J. Pharm. Biomed. Anal. 41 (2006) 393–399, https://doi.org/10.1016/J.JPBA.2005.11.037.

[46] S.A.J. Sulaiman, T. Bora, O.K. Abou-Zied, Spectroscopic characterization of the warfarin drug-binding site of folded and unfolded human serum albumin anchored on gold nanoparticles: effect of bioconjugation on the loading capacity, RSC Adv. 8 (2018) 7523–7532, https://doi.org/10.1039/C8RA00006A.

[47] B.A. Russell, P.A. Mulheran, D.J.S. Birch, Y. Chen, Probing the Sudlow binding site with warfarin: how does gold nanocluster growth alter human serum albumin? Phys. Chem. Chem. Phys. 18 (2016) 22874–22878, https://doi.org/10.1039/C6CP03428D.
[48] L. Galantini, C. Leggio, P.V. Konarev, N.V. Pavel, Human serum albumin binding ibuprofen: a 3D description of the unfolding pathway in urea, Biophys. Chem. 147 (2010) 111–122, https://doi.org/10.1016/j.bpc.2010.01.002.
[49] A. Das, R. Thakur, A. Dagar, A. Chakraborty, A spectroscopic investigation and molecular docking study on the interaction of hen egg white lysozyme with liposomes of saturated and unsaturated phosphocholines probed by an anticancer drug ellipticine, Phys. Chem. Chem. Phys. 16 (2014) 5368, https://doi.org/10.1039/c3cp54247e.
[50] Z. Wang, H. Sun, X. Yao, D. Li, L. Xu, Y. Li, S. Tian, T. Hou, Comprehensive evaluation of ten docking programs on a diverse set of protein–ligand complexes: the prediction accuracy of sampling power and scoring power, Phys. Chem. Chem. Phys. 18 (2016) 12964–12975, https://doi.org/10.1039/C6CP01555G.
[51] J.B.F. Lloyd, Synchronized excitation of fluorescence emission spectra, Nat. Phys. Sci. 231 (1971) 64–65, https://doi.org/10.1038/physci231064a0.
[52] R. Joshi, M. Jadhao, H. Kumar, S.K. Ghosh, Is the Sudlow site I of human serum albumin more generous to adopt prospective anti-cancer bioorganic compound than that of bovine: a combined spectroscopic and docking simulation approach, Bioorg. Chem. 75 (2017) 332–346, https://doi.org/10.1016/J.BIOORG.2017.10.013.
[53] S. Biswas, P.K. Chowdhury, Unusual domain movement in a multidomain protein in presence of macromolecular crowders, Phys. Chem. Chem. Phys. 17 (2015) 19820–19833, https://doi.org/10.1039/c5cp02674a.
[54] Lu. Gang, A. Sufen Ai, J. Li, Layer-by-layer assembly of human serum albumin and phospholipid nanotubes based on a template, Langmuir (2005), https://doi.org/10.1021/LA047771R.
[55] Q. Chen, X. Zhang, Y. Sun, M. Ritt, S. Sivaramakrishnan, X. Fan, Highly sensitive fluorescent protein FRET detection using optofluidic lasers, Lab on a Chip 13 (2013), https://doi.org/10.1039/c3lc50207d.
[56] Q. Wang, Y. Xiao, Y. Huang, H. Li, An important prerequisite for efficient Förster resonance energy transfer (FRET) from human serum albumin to alkyl gallate, RSC Adv. 6 (2016) 36146–36151, https://doi.org/10.1039/C6RA06920G.
[57] J. Tian, J. Liu, W. He, Z. Hu, A. Xiaojun Yao, X. Chen, Probing the binding of scutellarin to human serum albumin by circular dichroism, fluorescence spectroscopy, FTIR, Mol. Model. Method (2004), https://doi.org/10.1021/BM049668M.
[58] C. Dufour, O. Dangles, Flavonoid–serum albumin complexation: determination of binding constants and binding sites by fluorescence spectroscopy, Biochim. Biophys. Acta – Gen. Subj. 1721 (2005) 164–173, https://doi.org/10.1016/J.BBAGEN.2004.10.013.
[59] M. Amiri, K. Jankeje, J.R. Albani, Characterization of human serum albumin forms with pH. Fluorescence lifetime studies, J. Pharm. Biomed. Anal. 51 (2010) 1097–1102, https://doi.org/10.1016/j.jpba.2009.11.011.
[60] N. Tayeh, T. Rungassamy, J.R. Albani, Fluorescence spectral resolution of tryptophan residues in bovine and human serum albumins, J. Pharm. Biomed. Anal. 50 (2009) 107–116, https://doi.org/10.1016/J.JPBA.2009.03.015.